Title
Flame Height Measurement of Laminar Inverse Diffusion Flames

Journal
Combustion and Flame, 146(1-2)

Authors
Mikofski, Mark A.
Williams, Timothy C.
Shaddix, Christopher R.
et al.

Publication Date
2006

Peer reviewed

Title: Flame Height Measurement of Laminar Inverse Diffusion Flames

Authors: Mark A. Mikofski[1]

Timothy C. Williams[2]

Christopher R. Shaddix[2]

Linda G. Blevins[2]

Affiliations: [1]Microgravity Combustion Laboratory, University of California Berkeley

[2]Combustion Research Facility, Sandia National Laboratories, Livermore CA, 94550

Article Type: Full Length Article

Correspondence Address:

Linda G. Blevins

National Science Foundation

4201 Wilson Boulevard Suite 525

Arlington, VA 22230

Tel. (703) 292-8371

Fax (703) 292-9054

lblevins@nsf.gov

*Author is serving a temporary assignment at NSF in Arlington, VA.

Keywords: inverse diffusion flame, laminar, flame height, OH, laser induced fluorescence

Abstract

Flame heights of co-flowing cylindrical ethylene-air and methane-air laminar inverse diffusion flames were measured. The luminous flame height was found to be longer than the height of the reaction zone determined by planar laser-induced fluorescence (PLIF) of hydroxyl radicals (OH) because of luminous soot above the reaction zone. However, the location of the peak luminous signals along the centerline agreed very well with the OH flame height. Flame height predictions using Roper's analysis for circular port burners agreed with measured reaction zone heights when using values for the characteristic diffusion coefficient and/or diffusion temperature somewhat different from those recommended by Roper. The fact that Roper's analysis applies to inverse diffusion flames is evidence that inverse diffusion flames are similar in structure to normal diffusion flames.

Introduction

Inverse diffusion flames (IDFs) are similar to normal diffusion flames (NDFs), except that the relative positions of the fuel and oxidizer are exchanged. Soot and polycyclic aromatic hydrocarbons (PAH) form on the outside of the IDF in the fuel stream, experience temperature and mixture fraction histories different from those they would experience in NDFs, and escape unoxidized since they do not pass through the high temperature reaction zone [1-3]. Therefore, the study of IDFs may yield information about soot inception and growth and the formation of soot precursors, such as PAH [4-7].

Flame height is an important characteristic of co-flow laminar diffusion flames. Flame height measurements have been used to test models of flame structure [8-10] and to calculate residence times of soot particles [7,11]. The most commonly accepted definition of flame height is the distance from the burner to the position on the centerline where the fuel and oxidizer are in stoichiometric proportions [12]. The most frequently used method of measuring flame height is by visually inspecting the flame to determine the height of the blue reaction zone [3,11] since stoichiometric conditions occur on the oxygen side of a blue reaction zone caused by CO_2 and CH* chemiluminescence [13]. A more consistent measurement of flame height can be made by measuring the peak blue intensity on the flame axis recorded with a color charge-coupled device (CCD) camera and a line filter centered near 431 nm to enhance CH* luminescence and attenuate soot radiation [14,15]. Because the blue region in sooting NDFs is often difficult to detect, the luminous height of the yellow region has often been reported with the assumption that it is very close to the stoichiometric flame height in lightly sooting, non-smoking NDFs

[15-18]. However, for heavily sooting and smoking NDFs, the height of the luminous yellow region is above the reaction zone, yielding heights greater than the stoichiometric flame height [16,17,19,20]. Therefore, some researchers have used gas sampling on the centerline to measure flame height [12]. Since the flame temperature peaks at or near stoichiometric conditions, other researchers have reported the flame height by measuring the maximum temperature on the centerline using a thermocouple or Rayleigh scattering [2,9,10]. The position of the reaction zone can also be found by examining the position of planar laser-induced fluorescence of hydroxyl radicals (OH PLIF), since measurements of OH PLIF have shown that the maximum concentration of OH lies just to the lean side of the stoichiometric mixture in laminar diffusion flames [21]. Recently, flame height measurements have been made using OH PLIF in co-flowing cylindrical laminar IDFs of diluted ethylene and air [5].

Measurement of flame height in IDFs is complicated because soot forms in an annular region outside and above the flame and radiates, obscuring the blue reaction zone [4,6]. Therefore, measurement of stoichiometric flame height by OH PLIF is particularly suited to IDFs since visible images may not reveal information about the flame structure, and since gas sampling and temperature measurements along the centerline are intrusive and may alter the flame structure.

Theoretical consideration of flame height of laminar co-flow diffusion flames was first developed by Burke and Schumann. Although they made many assumptions in their analysis, they obtained good agreement between predicted and measured flame heights of NDFs and IDFs [22]. Several researchers expanded upon the work of Burke and Schumann by reducing the number of assumptions, but they did not apply their solutions

to IDFs [13,18-20,23-26]. Roper developed the theoretical correlations most commonly used for predicting NDF flame height [12,19,27]. However, the applicability of these correlations has not been demonstrated for IDFs. Wu and Essenhigh [2] compared theoretical flame shapes of IDFs based on the relations developed by Gosman *et al.* [26] to experiment and found reasonably good agreement. In their words, "…mathematically the normal and inverse flames are, indeed, essentially indistinguishable from each other, …with prediction of the alternate type simply obtained by treating the oxygen as fuel and the fuel as oxygen." Therefore, one would expect Roper's correlations to apply to IDFs with flame height increasing with rate of air flow.

The objectives of this paper are to (1) examine the relationship between flame heights of IDFs obtained from images of flame luminosity and OH PLIF, and (2) compare these with flame heights calculated using Roper's analysis [19].

Experimental Methods

The co-annular burner used to support laminar inverse diffusion flames in this study has been described in detail by Blevins *et al.* [4]. The burner consists of three concentric tubes as shown in Fig. 1. Air flows through a 1-cm diameter central tube. Fuel flows in the annulus between a 3-cm diameter tube and the central air tube. To prevent secondary flames from forming between the fuel and ambient air, nitrogen flows at a rate of 30 standard liters per minute (slpm, where standard conditions are 293 K and 101 kPa) through a second annulus formed between a 6.4-cm diameter outer tube and the 3-cm diameter tube. Table 1 lists the air and fuel flow rates for the methane and ethylene IDFs tested. Slight variations in the flow rates of nitrogen and fuel did not affect the

flame. To reduce flame instabilities caused by room air currents, the burner was surrounded by a metal shield with openings to admit laser light and to provide optical access for a camera.

A detailed description of the experimental method used to obtain the OH PLIF measurements is provided in ref. [6]. Hydroxyl radicals were excited by a laser sheet aligned vertically with the central axis of the burner and positioned from 3 mm below to 48.2 mm above the burner exit. A gated, intensified charge-coupled device (ICCD) camera with a 340 nm band-pass filter collected OH and PAH PLIF at a rate of 2.5 frames per second for 40 seconds totaling 100 frames. The ICCD camera stores the output for each pixel as a 16-bit absolute intensity value. Approximate stoichiometric flame heights were determined from the position of the OH layer by measuring the vertical distance from the burner exit to the maximum OH PLIF intensity on the centerline.

Measurements of luminous flame height were made from images of natural flame radiation recorded using the ICCD camera with the laser off and no filters. The ICCD camera without filters detects wavelengths of light between 200 nm and 900 nm. The images were collected at a rate of 2.5 frames per second for 8 seconds totaling 20 frames. Because several flames extended above the vertical domain of the ICCD camera, two sets of images were recorded, one with the burner in the original position, and another with the burner repositioned lower to record images of the flame from 22.7 mm to 73.9 mm above the burner exit.

Luminous flame heights were defined as the distance on the centerline from the burner exit to the point where flame luminosity is no longer visible to the eye. To

quantify this concept using the ICCD images, the intensity corresponding to the luminous height was defined to be 800 arb. units (out of 65535 maximum), determined to correspond to the location of the flame height as determined by comparison of the ICCD images to normal digital photographs for a few of the flames. This ICCD intensity level corresponded to roughly three times the average background intensity measured by the ICCD for pixels not exposed to the flame and located far from the image of the flame. The peak luminous intensity on the centerline of the visible images was also determined from the ICCD images and compared to the luminous heights and the OH-PLIF flame heights. The precision all flame height measurements was ±0.5 mm, and the precision in air flow rate measurements was ±0.1 slpm.

Calculations of flame height were based on the analytical solution derived by Roper for the height of the reaction zone for a circular port burner,

$$H/Q = \{4\pi D_0 \ln(1+1/S)\}^{-1}(T_0/T_f)^{0.67}, \quad (1)$$

where H is the diffusion flame height (cm), Q is the volumetric flow rate of fuel gas (cm^3/s) corrected to ambient temperature and pressure, D_0 is the diffusion coefficient at ambient temperature (cm^2/s), S is the ratio of the volume of air to volume of fuel gas for complete combustion, T_0 is the ambient temperature (K), and T_f is the characteristic temperature for calculation of diffusivity (K) [19]. The following modifications to Eq. 1 were made for IDFs: (1) air flow rate was used instead of fuel flow rate for Q, and (2) stoichiometric fuel to air volume ratio was used instead of stoichiometric air to fuel volume ratio for S. Since Roper's analysis requires the assumption that the diffusion coefficient of all species be equal, D_0 represents an effective diffusion coefficient. Roper *et al*. approximated D_0 as the binary diffusion coefficient of oxygen into nitrogen at

$T_0 = 293$ K ($D_0 = 0.20$ cm^2/s) [12]. However, other researchers have suggested that in NDFs fuel dominates diffusion and have found better agreement between measured and predicted flame heights when D_0 was approximated as the binary diffusion coefficient of the fuel into nitrogen [18,20].

Roper *et al.* measured the heights of many NDFs of different fuels and consequently determined that a linear relationship existed between the ratio H/Q and the term $[\ln(1 + 1/S)]^{-1}$ except for flames shorter than six times the diameter of the central fuel tube, which Roper hypothesized were shortened by axial diffusion, which was neglected in the analysis [12]. The measured linear relationship is consistent with Eq. 1 if D_0 and T_f are constant. Roper and colleagues determined the linear constant for this relationship and expressed it in the following correlation for NDFs of all fuels:

$$H/Q = (0.133 \text{ s/cm}^2)[\ln(1 + 1/S)]^{-1}. \quad (2)$$

Comparing Eqs. 1 and 2, Roper calculated the characteristic diffusion temperature, T_f, as 1500 K for NDFs and argued that this was a reasonable mean temperature for the flame region controlling diffusion.

Results and Discussion

An image of average OH and PAH PLIF from a 1.0 slpm air flow rate ethylene IDF is shown in Fig. 2(a). The OH PLIF signal and the approximate location of the OH flame height are marked. The surrounding PAH PLIF signal, present in the image, is also marked. Absolute luminous intensity and color visible images of the 1.0 slpm air flow rate ethylene IDF are shown in Figs. 2(b-c). The approximate location of the luminous flame height is indicated. It can be seen in Fig. 2(c) that the blue region of the flame

associated with CH* chemiluminescence and the reaction zone is masked by soot radiation. The flame appears qualitatively longer in the luminosity images of Figs. 2(b-c) than in the OH and PAH PLIF image of Fig. 2(a) because of the soot radiation surrounding and above the reaction zone. In Fig. 3, the absolute luminous intensity on the centerline is compared to the OH and PAH PLIF on the centerline from an ethylene IDF with an air flow rate of 1.0 slpm. The peak luminous height and the peak OH flame height are marked on the graphs. As in Fig. 2, Fig. 3 shows that the luminous flame height is greater than the stoichiometric flame height, determined by OH PLIF. The peak luminous height, also marked in Fig. 3, shows better agreement with the peak OH height.

The measured flame heights from both ethylene and methane IDFs are depicted in Figs. 4-5, respectively. The vertical bars on the luminous flame heights and OH PLIF heights represent one standard deviation in height. The standard deviation of the luminous ethylene flame heights increases with increasing air flow rates, reflecting an increase in the effects of buoyancy induced flame instabilities with increasing flame height [28]. The flame heights increase with increasing rate of air flow for both fuels. The luminous flame heights are greater than the flame heights from OH PLIF, since there is visibly radiating soot surrounding and extending above the reaction zone. Therefore, luminous flame heights of IDFs overestimate the height of the reaction zone.

The centerline peak ICCD luminosity height is shown for all flames in Figs. 4-5. The peak luminosity height corresponds very closely to the reaction zone determined by OH PLIF for the methane and ethylene IDFs investigated in this study. However, this finding should be interpreted carefully. The centerline luminosity consists mainly of CH* chemiluminescence and soot radiation. The use of an ICCD camera shows the soot

radiation projected on the centerline, even though the soot actually occurs in an annular ring around the centerline. If the IDF is a non-sooting or lightly sooting flame (as in the case of very low air flow rates or very low-sooting-tendency fuels like methane), then the CH* chemiluminescence should dominate. For sooting flames, the peak luminosity may be dominated by soot radiation projected onto the centerline. Soot radiation will depend strongly on the temperature of the soot. As sooting tendency of the fuel is increased or as the level of sooting is increased by increasing air flow, peak luminosity from soot radiation may occur lower in the flame due to radiant losses.

There is a discontinuity centered at an air flow rate of 1.6 slpm in the flame heights owing to an instability observed in the flame. This instability is also responsible for the large standard deviation at this flow rate. The flames in this study have Froude numbers between 0.2 and 0.4, which makes them slightly buoyant and near transition to momentum control. The smallest flames, which have the lowest Froude numbers and are therefore most buoyant, were observed to be the most stable. Therefore, it is unlikely that the instability was caused by the low fuel co-flow since it does not affect the most buoyant flames. The instability may have been caused by the exhaust fan ducting, which may have enhanced the natural flickering of the flame.

Flame heights predicted using Roper's analysis modified for IDFs are compared to OH PLIF measurements in Figs. 6-7. The dotted lines in Figs. 6-7 indicate predicted flame heights calculated from Roper's correlation (Eq. 2) [12]. When Roper's correlation is applied, flame heights are under predicted for all ethylene flames and almost all methane flames. This may be due to oxygen diffusing upward in the flames; the flames in this study are all shorter than six times the diameter of the central air tube, so axial

diffusion may be important [12]. The height of the methane flame with an air flow rate of 1.6 slpm is over predicted, but this flame was probably shortened by instability-induced mixing.

A modified Roper's correlation optimized for all OH PLIF flame heights from both ethylene and methane IDFs (disregarding the unstable methane flame with an air flow rate of 1.6 slpm) was generated by adjusting the coefficient of the correlation in Eq. 2. The resulting correlation,

$$H/Q = (0.157 \text{ s/cm}^2)[\ln(1 + 1/S)]^{-1}, \quad (3)$$

has parameter definitions the same as those in Eq. 1. The predicted flame heights calculated using Eq. 3, represented by solid lines in Figs. 6-7, agree with the OH PLIF measurements better than flame heights predicted with Eq. 2. However, the errors for ethylene flame heights are greater than the errors for methane flame heights. This suggests that a fuel-independent correlation may not exist for IDFs.

A least squares fit of the OH PLIF flame heights for only ethylene IDFs was used to generate a modified Roper's correlation for ethylene IDFs:

$$H/Q = (0.171 \text{ s/cm}^2)[\ln(1 + 1/S)]^{-1}. \quad (4)$$

The dashed line in Fig. 6 represents predicted flame heights calculated using Eq. 4. The difference between Eqs. 3 and 4 may be due to the effect of uncertainty in the value of the diffusion coefficient, D_0. Comparing Eqs. 1 and 4, using Roper's suggested diffusion coefficient, $D_0 = 0.20$ cm^2/s results in an average temperature of $T_f = 1033$ K, which is significantly lower than Roper's average temperature of $T_f = 1500$ K for normal diffusion flames. This suggests that a different diffusion coefficient should be used. Using the binary diffusion coefficient of ethylene into nitrogen calculated from Leonard-Jones

parameters at 293 K (D_0 = 0.153 cm^2/s [27]) yields a temperature of T_f = 1541 K, which is a much more reasonable average flame temperature.

It is useful to test the application of Roper's analysis using IDF OH PLIF flame heights reported in the literature. Flame heights measured by OH PLIF for ethylene/air IDFs from ref. [5] are compared to flame heights predicted by Eqs. 2-4 in Fig. 8. Roper's correlation (Eq. 2) under predicts the flame heights as it did for the ethylene IDFs in Fig. 6, perhaps due to oxygen diffusing upward; the heights of these IDFs are also less than six times the diameter of the central air tube, so axial diffusion may be important. Flame heights are also under predicted using Eq. 3, but they agree slightly better with the OH PLIF measurements than flame heights predicted with Eq. 2. This is further evidence that a single correlation may not be sufficient to predict flame heights of IDFs of different fuels. Nearly perfect agreement is obtained using Eq. 4, the modified correlation for ethylene IDFs. However, the calculated heights are slightly less than the measured heights when the fuel is most diluted. As the fuel mole fraction approaches one, the calculated heights better predict the measured heights. This is because increasing fuel dilution lowers the adiabatic flame temperature, effectively increasing the flame height since diffusion occurs more slowly at lower temperatures and the reactants will have more time to advect downstream. This implies that temperature differences between flames should be considered when applying Eq. 1.

It would be of interest to develop a strategy for applying Eq. 1 to IDFs. Since the average temperature, T_f, in Eq. 1, should vary from flame to flame, a good approximation of T_f is the average of the adiabatic flame temperature and the ambient temperature, T_0. This temperature will be used with Eqs. 1 and 4 to determine the diffusion coefficient,

D_0, that best fits the data. For ethylene, selecting an average temperature of $T_f = 1331$ K, which is the average of the adiabatic flame temperature (2369 K [27]) and $T_0 = 293$ K, results in a diffusion coefficient of $D_0 = 0.169$ cm^2/s. This diffusion coefficient is between the suggested extremes, but closer to the binary diffusion coefficient of ethylene into nitrogen, which is less than the binary diffusion coefficient of oxygen into nitrogen. This suggests that D_0 should be between the binary diffusion coefficient of oxygen into nitrogen and the binary diffusion coefficient of the fuel into nitrogen, but will be closer to the lesser of the two diffusion coefficients.

The preceding strategy was used to predict methane IDF flame heights. First a least squares fit of the OH PLIF flame heights for only methane (disregarding the unstable methane flame with an air flow rate of 1.6 slpm) was used to generate a modified Roper's correlation for methane IDFs:

$$H/Q = (0.150 \text{ s/cm}^2)[\ln(1 + 1/S)]^{-1}. \quad (5)$$

The predicted flame heights calculated using Eq. 5 are represented by a dashed line in Fig. 7. Comparing Eqs. 1 and 5, using an average temperature of $T_f = 1260$ K, which is the average of the adiabatic flame temperature of methane (2226 K [27]) and $T_0 = 293$ K, yields a diffusion coefficient of $D_0 = 0.200$ cm^2/s. This diffusion coefficient is between the binary diffusion coefficient of oxygen into nitrogen ($D_0 = 0.198$ cm^2/s [27]) and the binary diffusion coefficient of methane into nitrogen ($D_0 = 0.212$ cm^2/s [27]) calculated from Leonard-Jones parameters at 293 K, but closer to the binary diffusion coefficient of oxygen into nitrogen, which is the lesser of the two diffusion coefficients. Therefore, the strategy is effective. Based on the current experimental results, a first order approximation for D_0 can be given as follows:

$$D_{fuel} < D_{air},\ D_0 = D_{air} - 0.644*(D_{air} - D_{fuel})$$

$$D_{fuel} > D_{air},\ D_0 = D_{air} + 0.143*(D_{fuel} - D_{air}). \quad (6)$$

where D_{fuel} is the binary diffusion coefficient of the fuel into nitrogen and D_{air} is the binary diffusion coefficient of oxygen into nitrogen (0.198 cm^2/s [27]). However, longer IDFs should be measured and more fuels should be tested to verify this strategy. Nevertheless, the fact that Roper's treatment applies to IDFs agrees with previous papers that have postulated that IDFs are similar in structure to NDFs [1-3,5-7].

Conclusions

Flame heights of ethylene-air and methane-air laminar IDFs were measured for several air flow rates. The luminous flame height was found to be greater than the height of the reaction zone determined by OH PLIF because of luminous soot above the reaction zone; hence, luminous height is not an effective measure of flame height. In contrast, the location of the peak luminous emission along the flame centerline was found to give a good indication of stoichiometric flame height. Roper's analysis was found to provide good agreement with measured OH PLIF flame heights over the range of air flow rates examined in the present study and for literature data, when the following modifications were made to Eq. 1:

(1) rate of air flow was used instead of fuel flow for Q,

(2) fuel-to-air ratio was used instead of air-to-fuel ratio for S,

(3) the average of the adiabatic flame temperature of the fuel and ambient temperature was used for T_f, and

(4) a diffusion coefficient in between the binary diffusion coefficient of oxygen into nitrogen and the binary diffusion coefficient of the fuel into nitrogen, but closer to the lesser of the two diffusion coefficients, was used for D_0.

The fact that Roper's analysis applies to IDFs confirms that IDFs are similar in structure to NDFs.

Acknowledgments

This research was funded by the NASA microgravity combustion program under multiple contracts. Professor Carlos Fernandez-Pello and Dr. Amnon Bar-Ilan from U.C. Berkeley provided invaluable assistance. Sandia is a multi-program laboratory operated by Sandia Corporation, a Lockheed Martin Company, for the United States Department of Energy's National Nuclear Security Administration under Contract DE-AC04-94AL85000. Additional support was provided by a Laboratory Directed Research and Development project at Sandia National Labs.

References

[1]. J.H. Kent, H.G. Wagner, Zeitschrift Fur Physikalische Chemie-Wiesbaden 139 (1984) 59-68.

[2]. K.T. Wu, R.H. Essenhigh, Proc. Combust. Inst. 20 (1984) 1925-1932.

[3]. G.W. Sidebotham, I. Glassman, Combust. Flame 90 (3-4) (1992) 269-283.

[4]. L.G. Blevins, R.A. Fletcher, B.A. Benner, E.B. Steel, G.W. Mulholland, Proc. Combust. Inst. 29 (2003) 2325-2333.

[5]. E.J. Lee, K.C. Oh, H.D. Shin, Fuel 84 (5) (2005) 543-550.

[6]. C.R. Shaddix, C.W. Williams, L.G. Blevins, R.W. Schefer, Proc. Combust. Inst. 30 (2005) 1501-1508.

[7]. K.C. Oh, U.D. Lee, H.D. Shin, E.J. Lee, Combust. Flame 140 (3) (2005) 249-254.

[8]. A. D'anna, A. D'alessio, J. Kent, Combust. Sci. Technol. 174 (11-2) (2002) 279-294.

[9]. D.B. Makel, I.M. Kennedy, Combust. Sci. Technol. 97 (4-6) (1994) 303-314.

[10]. C.S. Mcenally, L.D. Pfefferle, A.M. Schaffer, M.B. Long, R.K. Mohammed, M.D. Smooke, M.B. Colket, Proc. Combust. Inst. 28 (2000) 2063-2070.

[11]. J. Du, R.L. Axelbaum, Combust. Flame 100 (3) (1995) 367-375.

[12]. F.G. Roper, C. Smith, A.C. Cunningham, Combust. Flame 29 (1977) 227-234.

[13]. R.E. Mitchell, A.F. Sarofim, L.A. Clomburg, Combust. Flame 37 (1980) 227-244.

[14]. P.B. Sunderland, B.J. Mendelson, Z.G. Yuan, D.L. Urban, Combust. Flame 116 (3) (1999) 376-386.

[15]. P.B. Sunderland, S.S. Krishnan, J.P. Gore, Combust. Flame 136 (1-2) (2004) 254-256.

[16]. K.P. Schug, Y. Manheimertimnat, P. Yaccarino, I. Glassman, Combust. Sci. Technol. 22 (5-6) (1980) 235-250.

[17]. K. Saito, F.A. Williams, A.S. Gordon, Combust. Sci. Technol. 47 (3-4) (1986) 117-138.

[18]. S.C. Li, A.S. Gordon, F.A. Williams, Combust. Sci. Technol. 104 (1-3) (1995) 75-91.

[19]. F.G. Roper, Combust. Flame 29 (1977) 219-226.

[20]. A.S. Gordon, S.C. Li, F.A. Williams, Combust. Sci. Technol. 141 (1-6) (1999) 1-18.

[21]. K.C. Smyth, P.J.H. Tjossem, A. Hamins, J.H. Miller, Combust. Flame 79 (3-4) (1990) 366-380.

[22]. S.P. Burke , T.E.W. Schumann, Industrial and Engineering Chemistry 20 (10) (1928) 998-1003.

[23]. J. Barr, B.P. Mullins, Fuel 28 (9) (1949) 200-207.

[24]. J.A. Fay, Journal of the Aeronautical Sciences 21 (10) (1954) 681-689.

[25]. J.F. Clarke, Proc. R. Soc. London, A 296 (1447) (1967) 519-545.

[26]. A.D. Gosman, W.M. Pun, A.K. Runchal, D.B. Spalding, M. Wolfshtein, Heat and Mass Transfer in Recirculating Flows, Academic Press, London, 1969.

[27]. S.R. Turns, An Introduction to Combustion: Concepts and Applications, McGraw-Hill, U.S.A, 2000, p. 656.

[28]. V.R. Katta, L.G. Blevins, W.M. Roquemore, Combust. Flame 142 (1-2) (2005) 33-51.

List of Tables

List of Figures

Figure 8 Flame heights measured by OH PLIF from ref. [5] compared to heights predicted by Roper's analysis.

Tables

Table 1. Flow Conditions

Fuel	Q_{fuel}[a]	Q_{air}[b]	V_{fuel}[c]	V_{air}[d]	V_{air}/V_{fuel}	$Re_{fuel,Dc}$[e]	$Re_{air,Dair}$[f]	$\Phi_{overall}$[g]	HRR_{air}[h]
	slpm	**slpm**	**cm/s**	**cm/s**					**W**
CH_4	3.8	1.2	10	26	2.5	120	170	30	70
		1.3		28	2.7		180	28	76
		1.6		34	3.3		230	23	93
		1.7		36	3.5		240	22	99
		1.8		38	3.8		250	20	110
		2.0		42	4.2		280	18	120
		2.2		47	4.6		310	17	130
		2.4		51	5.0		340	15	140
		2.6		55	5.4		370	14	150
		2.7		57	5.6		380	14	160
C_2H_4	2.7	1.0	7.2	21	2.9	170	140	39	64
		1.2		26	3.5		170	32	77
		1.4		30	4.1		200	28	90
		1.6		34	4.8		230	24	100
		1.8		38	5.3		250	22	120
		2.0		42	5.9		280	19	130
		2.2		47	6.5		310	18	140

[a] Q_{fuel}, volume flow rate of fuel (at 293 K and 101 kPa)

[b] Q_{air}, volume flow rate of air (at 293 K and 101 kPa)

[c] V_{fuel}, average cold-flow fuel velocity at the burner exit

[d] V_{air}, average cold-flow air velocity at the burner exit

[e] $Re_{fuel,Dc}$, Reynolds number based on the cold-flow conditions of the fuel at the burner exit and the hydraulic diameter, D_c = 2-cm

[f] $Re_{air,Dair}$, Reynolds number based on the cold-flow conditions of the air at the burner exit and the air tube diameter, D_{air} = 1-cm

[g] $\Phi_{overall}$, overall equivalence ratio, defined as the fuel-to-air ratio divided by the stoichiometric fuel-to-air ratio

[h] HRR_{air}, the estimated heat release rate based on the heating value of the fuel assuming all of the air reacts completely

Figures

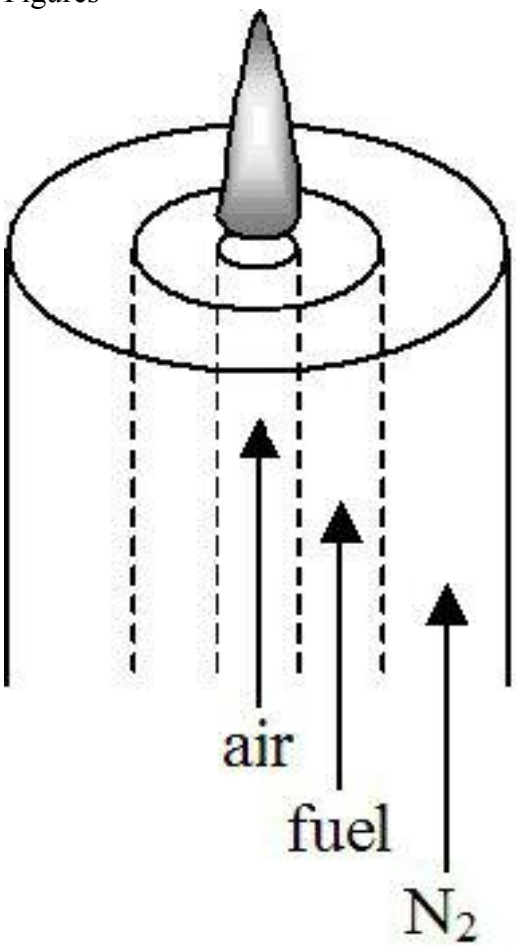

Fig. 1. Schematic diagram of burner.

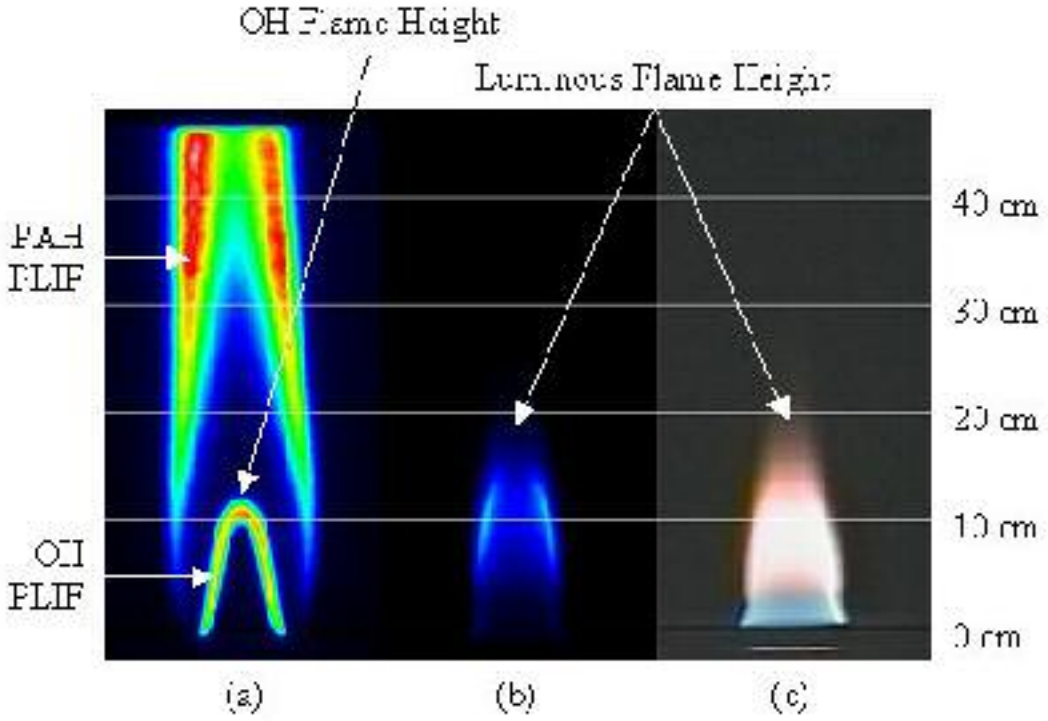

Fig. 2. Images of 1.0 slpm air flow rate ethylene IDF: (a) OH PLIF, (b) luminous flame (absolute intensity) from the ICCD, and (c) visible flame (color) recorded with a CCD camera (Panasonic WV-CP454) with a 16-mm focal length, f/8 Cosmicar lens.

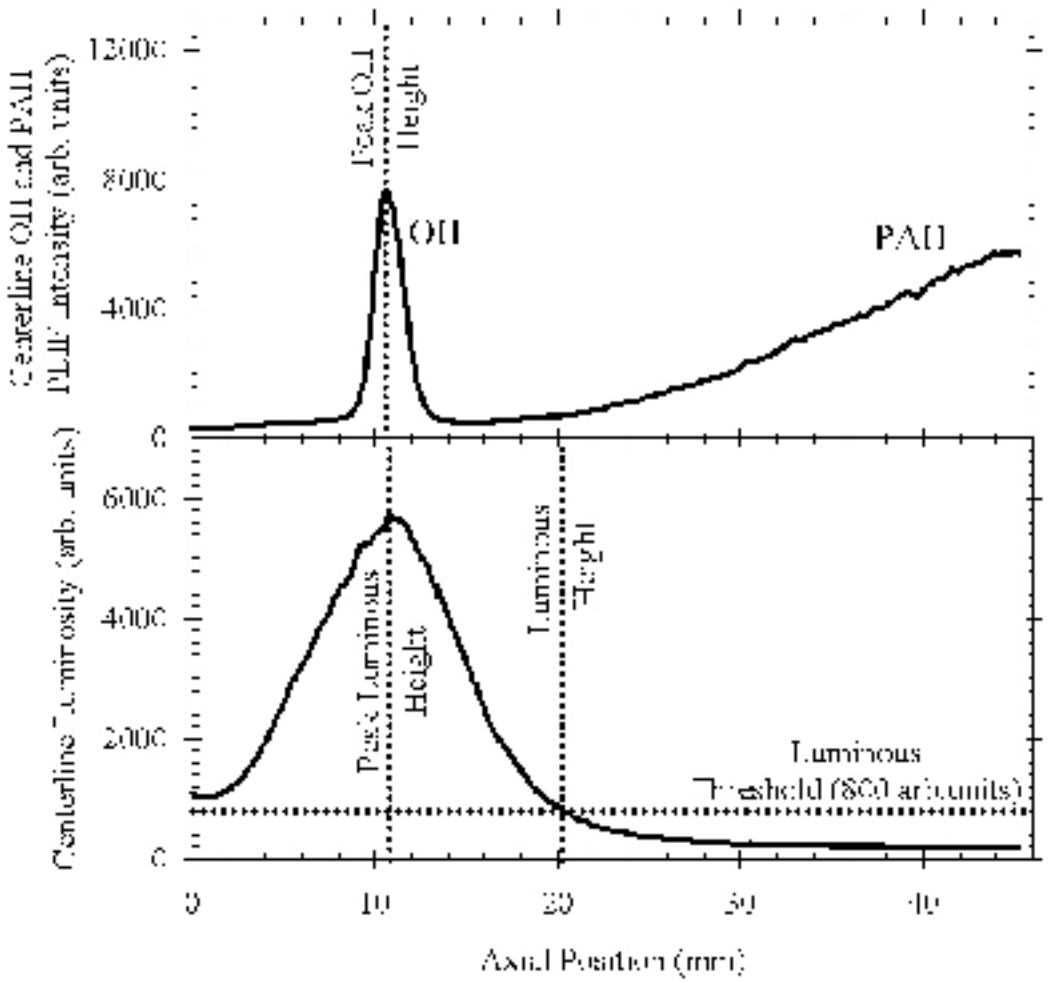

Fig. 3. Luminous intensity on the centerline compared with OH and PAH PLIF on the centerline from an ethylene IDF with an air flow rate of 1.0 slpm.

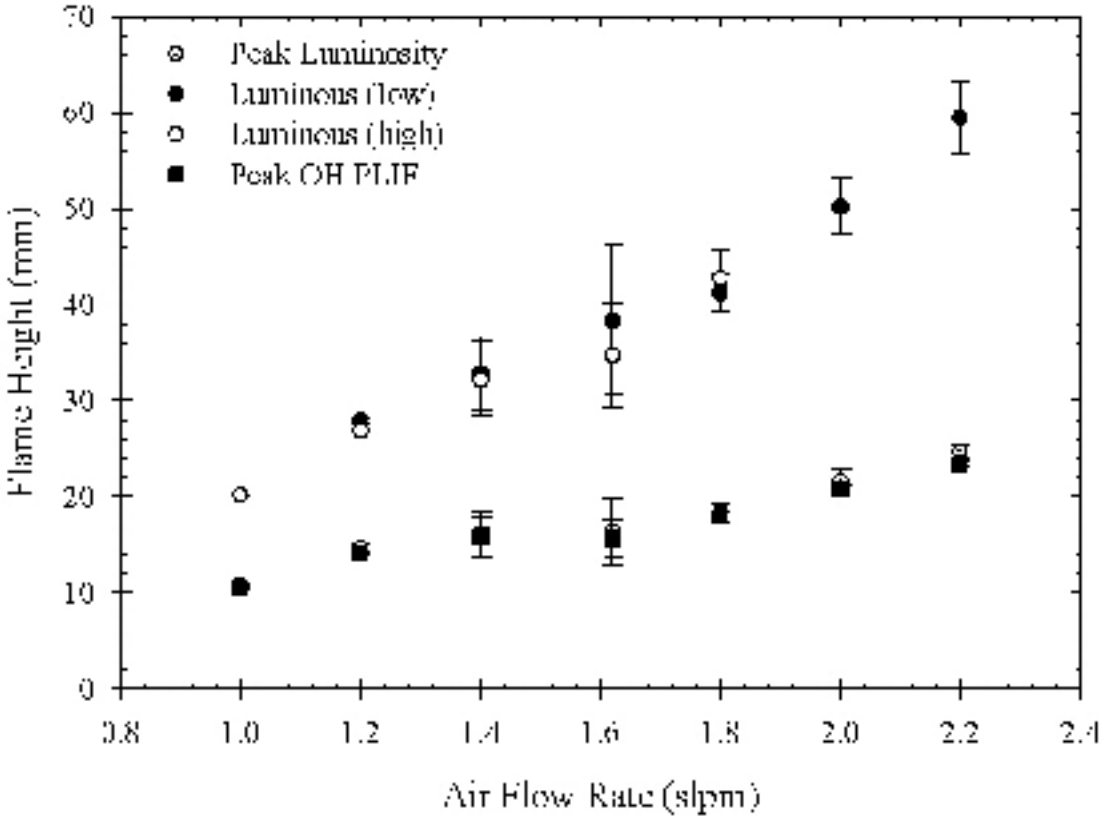

Fig. 4. Luminous and OH PLIF flame heights of ethylene IDFs. Luminous (low) shows flames with air flow rates from 1.2 slpm to 2.2 slpm with the burner in the lower position, and Luminous (high) shows flames with air flow rates from 1.0 slpm to 1.8 slpm with the burner in the upper position.

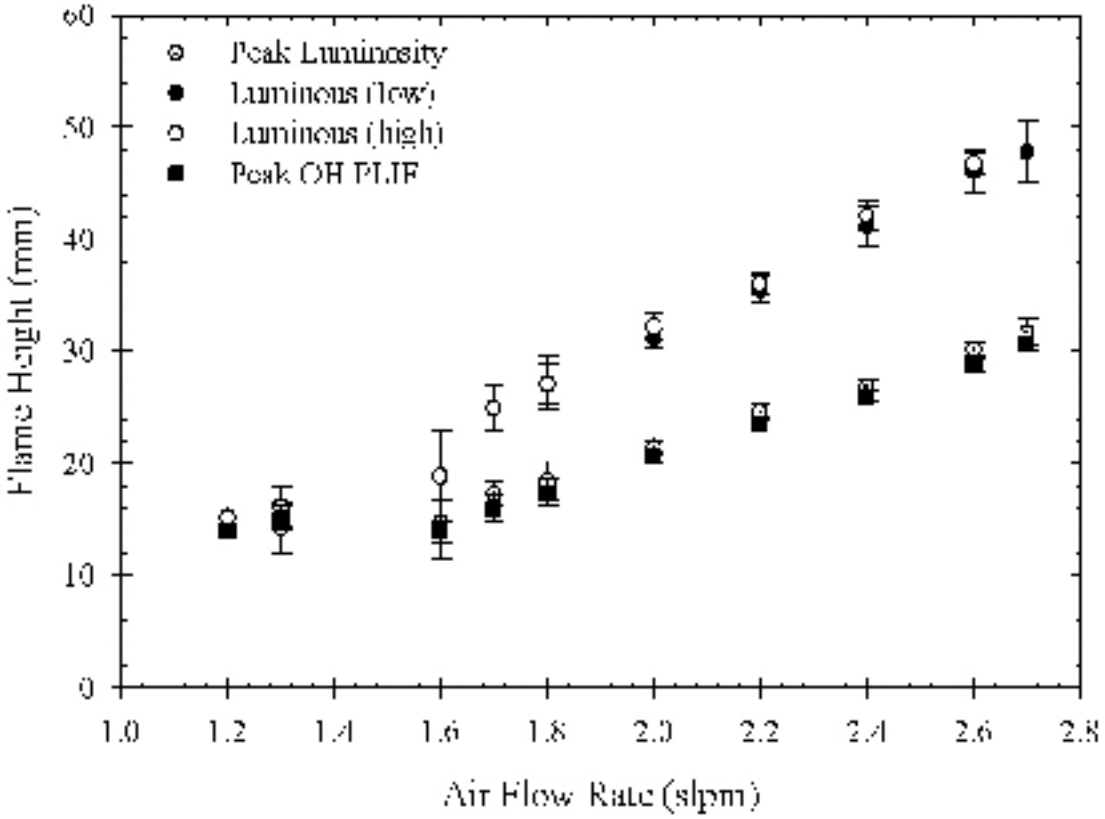

Fig. 5. Luminous and OH PLIF flame heights of methane IDFs. Luminous (low) shows flames with air flow rates from 1.8 slpm to 2.7 slpm with the burner in the lower position, and Luminous (high) shows flames with air flow from 1.2 slpm to 2.6 slpm with the burner in the upper position.

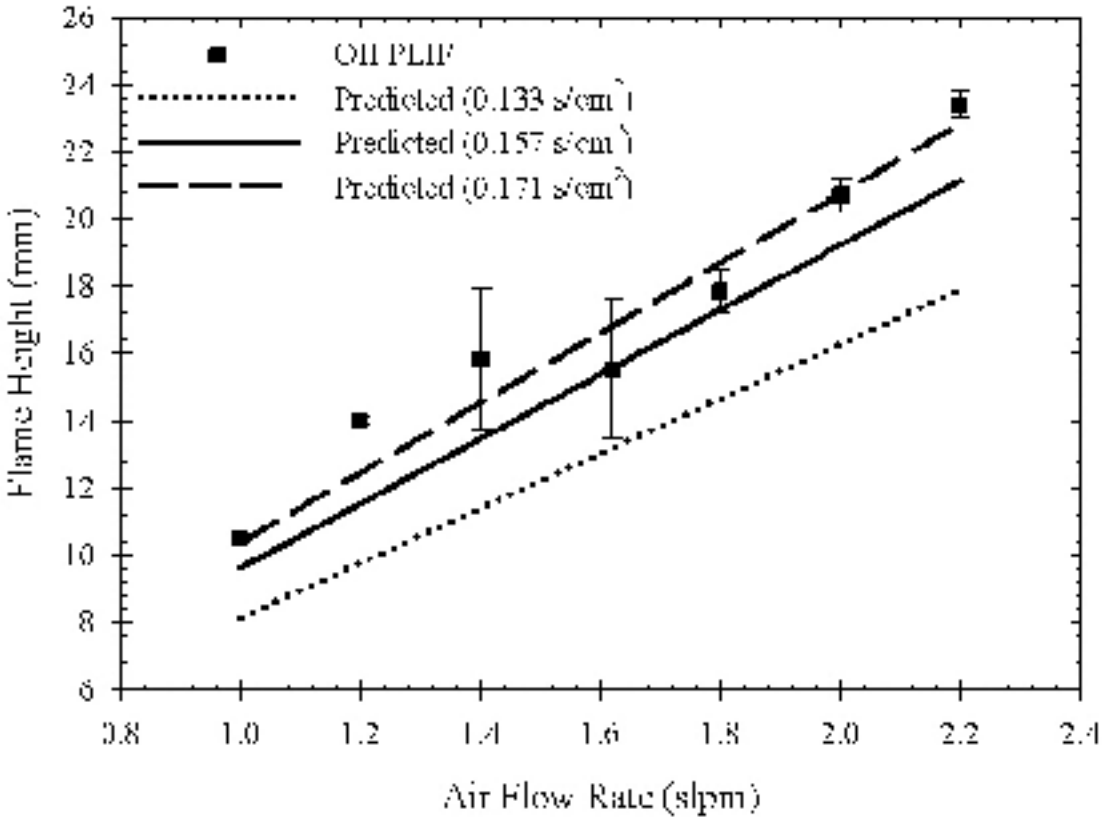

Fig. 6. Flame heights of ethylene IDFs predicted using Roper's analysis modified for IDFs compared to measured OH PLIF flame heights.

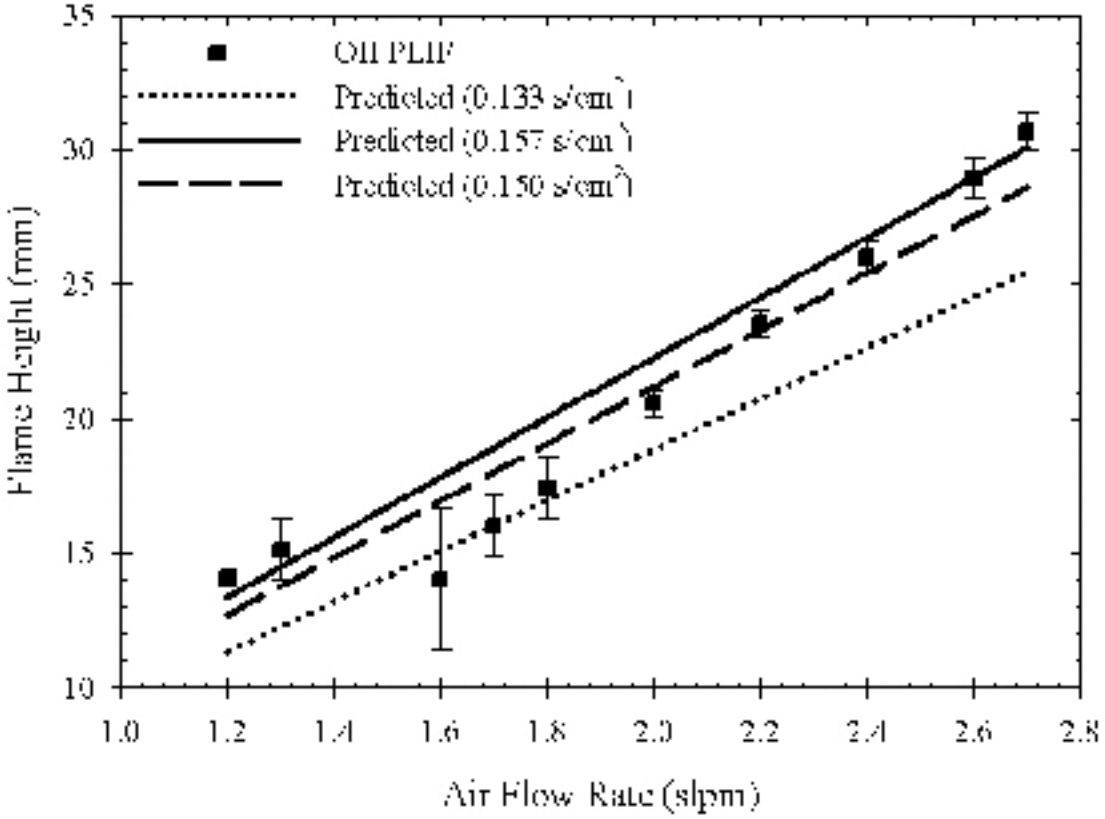

Fig. 7. Flame heights of methane IDFs predicted using Roper's analysis modified for IDFs compared to measured OH PLIF flame heights.

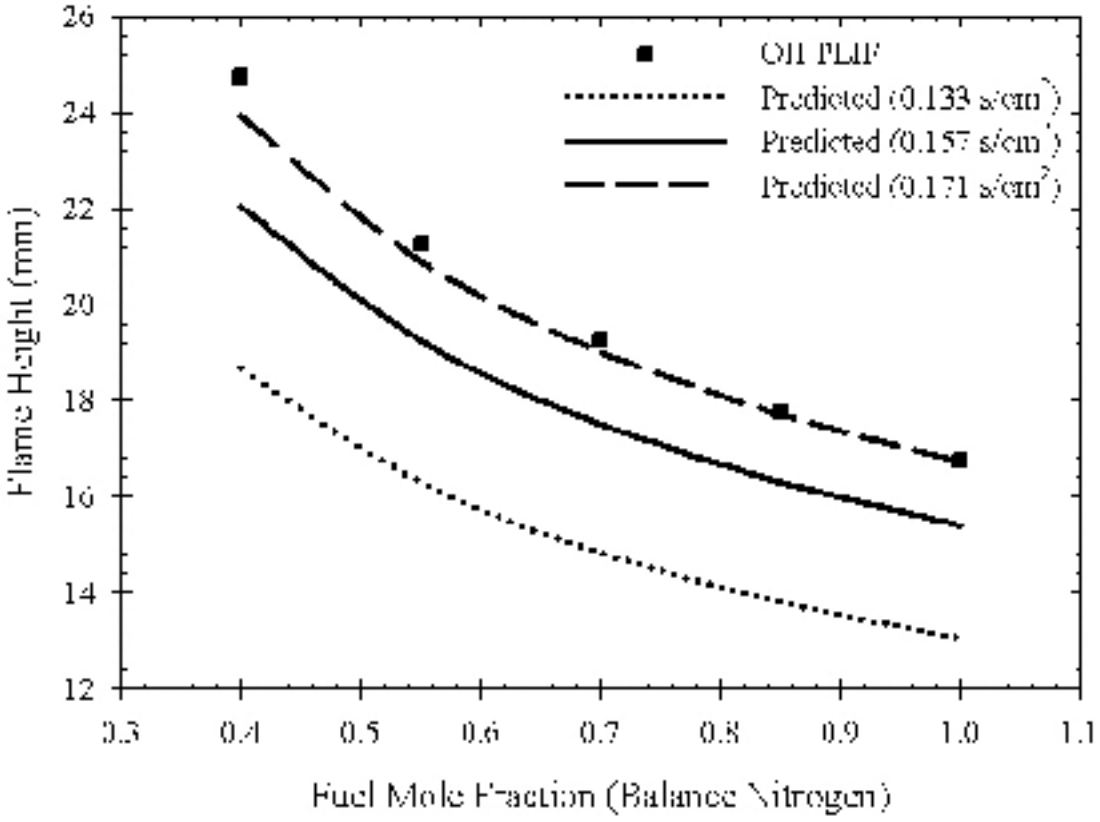

Fig. 8 Flame heights measured by OH PLIF from ref. [5] compared to heights predicted by Roper's analysis.